Journal of Materials Chemistry C

RSC Publishing

PAPER

View Article Online
View Journal | View Issue

A versatile ultra-thin Au nanomesh from a reusable anodic aluminium oxide (AAO) membrane†

Cite this: *J. Mater. Chem. C*, 2013, **1**, 5330

Sang-Joon Park,[ab] Hee Han,[a] Hyun Rhu,[a] Sunggi Baik[b] and Woo Lee*[a]

We demonstrated multiple replications of versatile ultra-thin Au nanomeshes from a single porous anodic aluminium oxide (AAO) membrane as a reusable replication master. A bilayered film of Ag and Au was sequentially deposited on nanoporous AAO (*i.e.*, Au/Ag/AAO), in which the Ag layer sandwiched in-between the Au layer and AAO serves as a sacrificial layer for separating the Au film from the oxide membrane during selective wet-chemical etching of Ag in HNO_3 solution. The structure of the separated Au film is characterized by a free-standing nanomesh, the hole array pattern and pitch distance of which are defined by the AAO replication master. Ultra-thin Au meshes can be transferred onto substrates of choice without any structural failure. On the other hand, our repeated replication experiments have revealed that a single porous AAO replication master can be reused more than 30 times without significant structural changes. In the present work, we demonstrated the versatility of replicated Au nanomeshes in various nanofabrications, including preparation of extended arrays of Si nanowires (SiNWs) by metal-assisted chemical etching of silicon wafers and surface patterning of polymeric substrates with sub-100 nm resolution. The applicability of Au meshes as an electrode for flexible devices was manifested by comparable resistance values of Au meshes on the polymer substrate, *viz.*, polyethylene terephthalate (PET), to a continuous Au film and stable *I–V* behaviours regardless of its bending state. The present approach of multiple replications of metal meshes from a single AAO membrane can be readily extended to other metallic materials and is time- and cost-effective compared to conventional lithographic methods.

Received 23rd May 2013
Accepted 2nd July 2013

DOI: 10.1039/c3tc30970c

www.rsc.org/MaterialsC

Introduction

Noble metal nanomeshes (*i.e.*, thin films with perforated arrays of periodic nanoholes) have recently been paid huge attention due to their potential applications in plasmonics,[1,2] photovoltaics,[3–5] biosensing,[3,6,7] cell adhesion and migration,[8] metal-assisted chemical etching (MaCE) of silicon[9–12] by virtue of their excellent manipulation, concentration, collection, and transmission of light at the sub-wavelength scale, high conductivity, and chemical and physical stability. To date, various patterning methods have been employed to fabricate metal nanomeshes: electron-beam lithography (EBL),[13] focused-ion beam (FIB) milling,[7] nanosphere lithography (NSL),[4,8] soft lithography,[1,3] nanoimprint lithography (NIL),[6] and block-copolymer-based lithography.[9,14] These techniques render a well-controlled patterning at the nanoscale. However, they are achieved through complicated and laborious processes (*e.g.*, sacrificial polymer layer patterning, resist removal, oxygen plasma treatment, polymer curing, master preparation, reactive ion etching, *etc.*).

As an alternative for overcoming the drawbacks of conventional methods for metal nanomesh fabrications, we developed a non-lithographic method for gold (Au) nanomeshes using a reusable nanoporous anodic aluminium oxide (AAO) membrane with the aid of a sacrificial Ag layer. AAO has been extensively employed for fabricating two-dimensional (2D) extended arrays of diverse functional nanostructures because of easy tunability of the pore diameter (D_p = 20–400 nm), interpore distance (D_{int} = 60–500 nm), pore density ($\rho = 10^8$ to 10^{10} cm^{-2}), and shape of pores by controlling electrochemical parameters (*viz.*, anodising electrolytes and voltages) or by adopting a pre-patterned aluminium substrate.[15–20]

Fabrication methods of large-scale metal meshes up to several square centimeters have been previously reported, wherein nanoporous AAO was utilized as a sacrificial template for replicating metal meshes by selective chemical dissolution of AAO from a metal-coated AAO membrane.[10–12] Inspired from the previous work, we established a highly robust alternative process of fabrication of metal nanomeshes, in which an Au

[a]*Korea Research Institute of Standards and Science (KRISS), Yuseong, Daejeon, 305-340, Korea. E-mail: woolee@kriss.re.kr*

[b]*Department of Materials Science and Engineering, Pohang University of Science and Technology (POSTECH), Hyoja-dong, Pohang, 790-784, Korea*

† Electronic supplementary information (ESI) available: Schematic diagram for transfer of an Au mesh on a substrate, electrical measurement configuration for the Au mesh and film on PET, EDS mapping results on Au meshes, SEM micrographs of the bottom side of AAO etched in HNO_3 (60%) for varied etching times (t_{etch}) from 0 to 70 min and TEM images of Si(001) NWs. See DOI: 10.1039/c3tc30970c

nanomesh was conveniently obtained by selectively removing the Ag sacrificial layer from the Au/Ag-coated AAO membrane. The resulting Au mesh was used not only as an etching catalyst in MaCE of silicon wafer for the preparation of extended arrays of Si nanowires (SiNWs), but also as a lithographic mask for patterning of a polymeric substrate (*viz.*, polystyrene (PS) in the present study), demonstrating the versatility of the replicated Au mesh. The primary merit of our approach over conventional AAO-based nanofabrication methods is that a single porous AAO master can be used several times for replicating multiple copies of metal nanomeshes, saving time and cost of the starting AAO material by anodisation of aluminium.

Experimental

Free-standing AAO membrane preparation

Free-standing self-ordered porous anodic aluminium oxide (AAO) membranes employed for the fabrication of Au meshes were prepared by anodising aluminium (Al) under potentiostatic conditions. Mirror-finished Al substrates were obtained by electrochemically polishing Al (typical diameters = 2 or 4 cm) in 1 : 4 mixture solution of 65% $HClO_4$ and 99.5% ethanol in order to prevent local electrochemical events associated with surface roughness. The resulting Al substrates were anodised in 0.3 M $H_2C_2O_4$ (7 °C) at 40 V for 24 h. After anodisation, the remaining Al substrate was selectively etched away by using an aqueous mixture solution of 3.4 g $CuCl_2 \cdot 2H_2O$, 50 mL of 38 wt% HCl, and 100 mL de-ionized (DI) water. In order to utilize the self-ordered hole pattern at the bottom side of the resulting porous AAO in the preparation of the Au mesh, the barrier layer at the pore bottom of AAO was opened, and subsequently pores were widened to a desired diameter (D_p) by using 5 wt% H_3PO_4 (29 °C).[19] The average interpore distance (D_{int}) of the prepared AAO membranes turned out to be 100 nm.

Fabrication of Au nanomeshes by utilizing a reusable AAO membrane

As depicted in Fig. 1a, multiple copies of Au nanomeshes (*viz.*, an Au thin film perforated with ordered arrays of nanoholes) were replicated from a single AAO membrane (see also ESI, Scheme S1†). Firstly, a 10 nm-thick Ag and a 25 nm-thick Au layer were sequentially deposited on the bottom surface of the free-standing AAO membrane by using a sputter coater (208HR, Cressington, UK). During metal deposition, the sample stage was oriented at a glancing angle of *ca.* 10° with respect to the sputter source for the minimization of undesired deposition of metal nanoparticles (NPs) on the surface of the AAO pore wall and rotated at a rate of 100 rpm. Fig. 1b shows a photograph of the resulting Au/Ag-coated AAO membrane, wherein AAO was prepared by anodising an Al disc of 4 cm diameter. Secondly, the Au nanomesh, replicating the spatial hole ordering of AAO, was separated from the AAO membrane by selective removal of the sacrificial Ag layer in 65 wt% HNO_3 solution at room temperature (RT). Owing to the low surface energy of metal layers (*i.e.*, Au and Ag), the Au/Ag-coated AAO membrane was floated on the surface of the Ag-etching solution (*i.e.*, HNO_3). The Ag layer was selectively etched away within 10 min without chemical dissolution of the AAO replication master: the separated Au mesh remains floating on the surface of the Ag-etching solution, while the AAO membrane sinks into the solution. Finally, the HNO_3 solution was replaced with diluted aqua regia and DI-water in order to remove undesired loosely bound metal nanoparticles at the edges of the nanoholes of the Au mesh and to rinse the resulting Au mesh, respectively. The Au nanomesh floating on the surface of DI-water was transferred onto a desired substrate. We adopted Si and polyethylene terephthalate (PET) substrates as a rigid and flexible substrate, respectively. Fig. 1c and d present photographs of the resulting Au-mesh-loaded Si(001) and PET substrates, respectively. In the present work, a single AAO membrane can be used as a replicating master for more than 30 times for the preparation of Au nanomeshes. In order to ensure complete removal of Ag, X-ray spectroscopy (EDS) analyses on our Au nanomesh loaded on the Si substrate were performed using a scanning electron microscope (SEM; Hitachi S-4800) equipped with a Bruker AXS XFlash 4010 SDD EDS detector with an energy resolution of 125 eV.

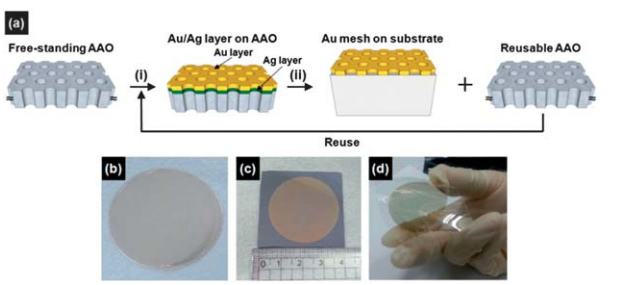

Fig. 1 (a) Schematic diagram for fabrication of an Au nanomesh by utilizing reusable AAO through (i) sequential deposition of an Ag and Au layer on a free-standing AAO membrane and (ii) selective dissolution of an Ag sacrificial layer and transfer of the separated Au mesh onto a substrate. Thicknesses of Au and Ag layers were 25 and 10 nm, respectively. Photographs of (b) an Au/Ag-coated AAO membrane and an Au nanomesh transferred onto (c) a rigid Si substrate and (d) a flexible PET substrate.

Si nanowire (SiNW) arrays *via* metal-assisted chemical etching (MaCE) of Si

Extended arrays of SiNWs were prepared by performing metal-assisted chemical etching (MaCE) of silicon wafer by utilizing Au meshes as an etching catalyst (Scheme 1a). Boron-doped Si(001) substrates (ρ = 1–10 Ω·cm) were cleaned in a Piranha solution (98% H_2SO_4–30% H_2O_2, v/v = 4/1), rinsed with a copious amount of DI-water, and finally dried under a strong stream of nitrogen. Au-mesh-loaded Si(001) was chemically etched by immersing the sample into an etching solution (46 wt% HF–35 wt% H_2O_2, v/v = 2 : 1) instantly after dipping into absolute ethanol.[11] Microscopic characterization of the SiNWs was carried out using a field emission scanning electron microscope (FE-SEM, Hitachi S-4800) and a transmission electron microscope (TEM, Tecnai F30, FEI, USA) operated at a primary beam energy of 300 kV.

Patterning of polystyrene (PS) by reactive ion etching (RIE)

An Au mesh was used as a lithographic mask for patterning of a polystyrene (PS) film by capacitively coupled plasma reactive ion

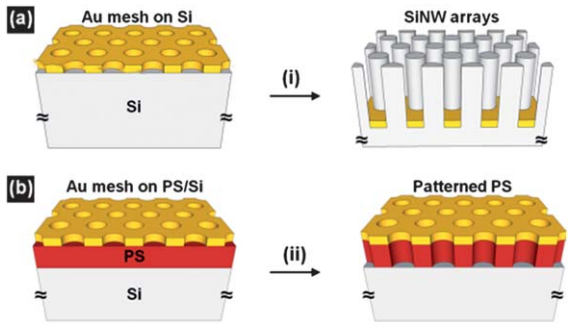

Scheme 1 Schematics for the fabrication of (a) SiNW arrays *via* metal-assisted chemical etching (MaCE) of Si by utilizing the Au mesh as an etching catalyst and (b) patterning of the polystyrene (PS) layer through reactive-ion etching (RIE) of PS by employing the Au mesh as an etching mask, respectively.

etching (CCP-RIE) (see Scheme 1b). PS was spin-coated on the HF-treated Si(001) substrate. The thickness of PS was measured to be 40 nm. Prior to the transfer of the Au mesh onto the PS-coated Si(001), the surface of the PS film was subjected to oxygen plasma treatment (45 W) for 10 s to attain sufficient hydrophilicity, which allows reliable transfer of the Au mesh onto the originally hydrophobic PS surface without folding or fissuring of the ultra-thin Au mesh. Au-mesh-loaded PS/Si(001) substrates were etched by CCP-RIE, in which 5-sccm O_2 (99.999%) was used as an etching gas. The RIE chuck power (*i.e.* CCP power) and chamber pressure were 50 W and 5 mTorr, respectively.

Current–voltage (*I–V*) measurements of an ultra-thin Au mesh on a flexible polyethylene terephthalate (PET) substrate

In order to investigate the potential application of our mesh to flexible electronic devices, we performed current–voltage (*I–V*) measurements on the as-prepared Au-mesh-loaded polyethylene terephthalate (PET) substrate using a semiconductor parameter analyzer (Keithley, 4200-SCS). Electrical contacts on the Au mesh were formed by using silver (Ag) paste; the distance between two Ag contacts was 3 cm. An Au-coated tungsten probe tip was utilized in this work. *I–V* characteristics of the samples were measured on a 25 nm-thick Au mesh while bending and releasing the samples; the bending radius of curvature was 1.66 cm. Bending of samples was achieved by loading a bent substrate in a plastic box (see ESI, Fig. S1†). As a control experiment, *I–V* curves of a 25 nm-thick Au continuous film on a PET substrate were also measured under the same bending conditions. The resistance values were obtained from fitting results of the measured *I–V* curves. A bending fatigue test was performed to examine the reliability of the Au mesh as a flexible electrode by measuring the *I–V* curves of the sample after repeatedly bending it inward and outward.

Results and discussion

Au nanomesh from reusable AAO

Multiple copies of Au meshes were replicated from a single AAO membrane as a replication master by taking advantage of selective removal of an Ag layer in Au/Ag-coated AAO in HNO_3 solution. In the present replication protocol, Au meshes can be obtained without causing any significant damage of the AAO replication master. According to EDS analyses on the present Au nanomeshes overlying on the Si substrate, Ag turned out to be completely etched away (see ESI, Fig. S2†). Fig. 2a–c display representative scanning electron microscopy (SEM) images of the 25 nm-thick Au nanomesh transferred onto the Si(001) substrate. As can be seen in SEM images, the Au mesh exhibits the hexagonally arranged nanohole arrays, indicating high fidelity in the transfer of the ordered hole array pattern of the porous AAO replication master. The hole diameter was found to be 58.8 ± 1.7 nm, which is smaller than the pore diameter ($D_p = 64.6 \pm 1.7$ nm) of the AAO replication master (see Fig. 3). The reduced hole size can be attributed to the closure effect, that is, progressive reduction of the hole size of a metal mesh as a function of metal sputtering time.[21] Fig. 2d presents the SEM

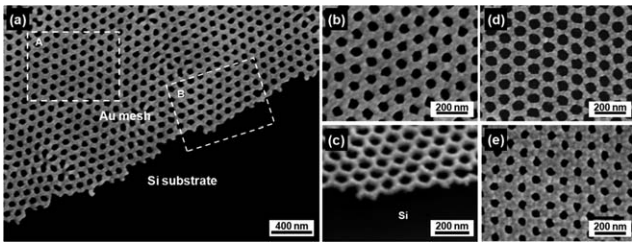

Fig. 2 SEM images of an Au nanomesh transferred onto Si(001) wafer: (a) top-view at the edge of the Au mesh, (b) magnified view of the area denoted as A in (a) and (c) 45°-tilt-view of the squared area denoted as B, (d) top-view of the Au mesh replicated from 30-times reused AAO, and (e) top-view of the Au mesh with hole arrays of 48.2 nm in diameter.

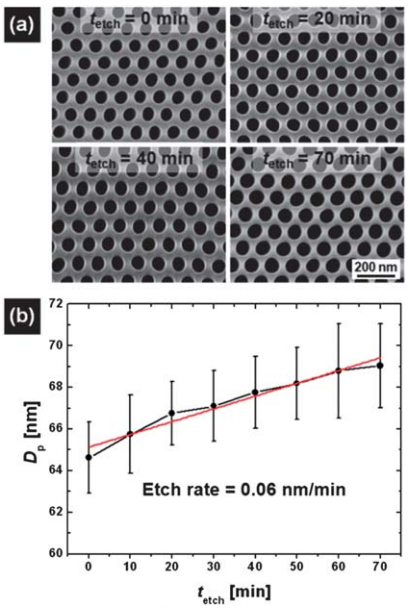

Fig. 3 (a) Representative SEM images of the bottom side of the through-hole AAO membrane which was etched in 60 wt% HNO_3 for varied etching times (t_{etch}) for 0, 20, 40, and 70 min at room temperature (RT) and (b) variation of pore diameter (D_p) as a function of t_{etch} and the linear fit (red trace).

image of the 30th Au mesh replica obtained from the AAO that was used for the preparation of the Au mesh shown in Fig. 2a–c. As clearly seen in Fig. 2d, even after reuse of AAO for 30 times, the replicated Au mesh exhibits well-defined hole array patterns of AAO, although the hole diameter was increased to 70.4 ± 2.1 nm. The present result clearly demonstrates the reusability of AAOs in our process. The hole size of Au meshes can be further adjusted by employing an AAO replication master with different pore diameters (D_p). Fig. 2e shows an SEM micrograph of an Au mesh fabricated from AAO with $D_p = 53.4 \pm 2.1$ nm. The hole diameter of the prepared Au mesh was measured to be 48.2 ± 1.4 nm. This indicates that the hole diameter of Au meshes can be readily tuned by adopting AAOs with different pore diameters. Previously, we successfully prepared Au membranes with arrays of micrometer-sized holes from a macroporous Si substrate, although the approach was slightly different from the present method.[22] Therefore, Au meshes with micrometer-sized holes and with different thicknesses could be easily replicated from recently reported AAOs with micro-sized hole arrays.[23]

Variation in pore diameter of AAO (D_p) depending on HNO_3-etching time (t_{etch})

Reusability of the AAO membranes was proven by investigating the rate of pore widening during the pore wall etching in 60 wt% HNO_3 (RT). Surface SEM images in Fig. 3a show the evolution of pore diameter (D_p) as a function of etching time (t_{etch}) (see also ESI, Fig. S3†). As confirmed in Fig. 3a, the pore diameter (D_p) of AAO was found to be only slightly increased even after an extended wet-chemical etching for $t_{etch} = 70$ min. In order to explore quantitative information on the pore wall etching rate, we carried out real-space image analyses on SEM micrographs measured from AAOs etched in 60 wt% HNO_3 solution for different periods of etching times (t_{etch}) from 0 to 70 min at an interval of 10 min (see Fig. S3†) by using a standard image processing package (*e.g.*, ImageJ; 1.36b, NIH, USA). Fig. 3b shows the results of pore size analyses of the HNO_3-etched AAOs as a function of etching time (t_{etch}). It turned out that the pore diameter (D_p) of AAO increases at a rate of 0.06 nm min^{-1}. In our typical experiments, an Au mesh was separated from an AAO replication master within 10 min, which may result in 0.6 nm increase of the pore diameter (D_p). Accordingly, AAO can be used repeatedly over 30 times, ensuring the reusability of the AAO.

Fabrication of silicon nanowire (SiNW) arrays by using Au meshes as an etching catalyst

As mentioned earlier, Au meshes can be utilized as an etching catalyst for the preparation of extended arrays of silicon nanowires (SiNWs). We performed metal-assisted chemical etching (MaCE) of Si by immersing the Au-mesh-loaded Si(001) wafer into the mixture solution of 46 wt% HF and 35 wt% H_2O_2. In MaCE of Si, metal acts as an etching catalyst for the reduction of the oxidant (*i.e.*, $H_2O_2 + 2H^+ + 2e^- \rightarrow 2H_2O$) by using electrons withdrawn from the underlying Si (*viz.*, injection of positive holes (h^+) into the valence band (VB) of Si) through the interface between metal and Si. Oxidative dissolution of Si by HF occurs at the junction between metal and Si (*i.e.*, $Si + h_{VB}^+ + 6F^- \rightarrow SiF_6^{2-} + 3e_{CB}^-$), allowing continuous forward movement of the etching front (*i.e.*, metal–Si interface). In other words, etching of Si is brought about from the interplay between the oxidation of Si through the injection of positive holes (h^+) and the elimination of oxidized silicon atoms by HF through breaking of their back bonds.[11,12,24] Fig. 4 shows SEM images of the resulting uniform SiNW arrays with hexagonal arrangement. As clearly shown in Fig. 4, our approach enables one to synthesize extended arrays of SiNWs with highly uniform length and diameter. In this approach, the length of NWs depends on MaCE time (see ESI, Fig. S4†). It is well established that the surface roughness of SiNWs formed by MaCE depends sensitively on the etchant composition (*i.e.*, the mixing ratio of HF and H_2O_2).[10] Under the present MaCE conditions (*i.e.*, HF : H_2O_2 = 2 : 1 in v/v), we can prepare single crystalline SiNWs with smooth surface morphology with sub-nm surface roughness (see ESI, Fig. S4†).

Patterned polystyrene (PS) prepared by utilizing Au mesh etching mask

Apart from etching catalyst in MaCE of Si, the Au mesh was used as an etching mask for patterning of polymeric films (*e.g.*, polystyrene; PS). For this purpose, capacitively coupled plasma reactive ion etching (CCP-REI) was performed on a PS-coated Si substrate (thickness of PS = 40 nm). O_2 was adopted as an etching gas. Fig. 5 shows SEM images of the resulting patterned PS. As shown in Fig. 5, a hexagonally ordered hole pattern of the Au mesh was successfully transferred onto the PS layer as a result of RIE of the polymer through an Au mesh mask, indicating the adaptability of the present Au mesh as a large-area lithographic mask for nanoscale patterning. Moreover, our approach can be readily applied to arbitrary substrates, provided that materials to be patterned exhibit an acceptable etching selectivity against the Au mesh mask.

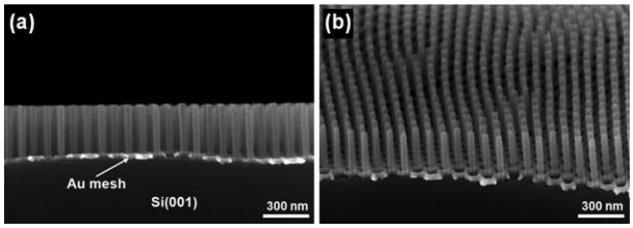

Fig. 4 Representative SEM images of SiNW arrays fabricated by MaCE of the Si(001) substrate in a mixture solution of HF and H_2O_2 [HF : H_2O_2 = 2 : 1 in v/v]: (a) cross-sectional view and (b) tilt-view.

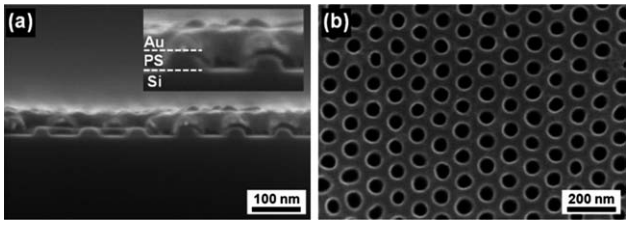

Fig. 5 SEM images of patterned PS (40 nm) by O_2-RIE through an Au mesh mask: (a) cross-sectional view and magnified image (inset) without removal of the Au mesh and (b) top-view after removing the Au mesh using aqua regia.

Au mesh as an electrode for flexible electronic devices

In order to demonstrate the applicability of our Au mesh to flexible electronic devices as an electrode, we performed current–voltage (*I–V*) measurements on Au meshes transferred on a flexible polymer substrate, *i.e.*, polyethylene terephthalate (PET) under bent and released states. Fig. 6a presents the resulting *I–V* curves of Au nanomeshes and continuous thin Au films of the same thickness (*i.e.*, 25 nm). As can be seen in Fig. 6a and summarized in Table 1, the resistance values of the Au mesh are comparable to those of the continuous Au film, although the former are somewhat higher than the latter. Stable *I–V* behaviors of the Au mesh were observed irrespective of its bending state. It has recently been reported that the nanohole-structured Cu electrode exhibited significantly improved mechanical and electrical reliability as a flexible electrode.[25] In light of this, we examined the reliable applicability of the present Au mesh as a flexible electrode. To this end, we investigated the variation in resistance of the Au mesh and the continuous film by measuring the *I–V* curves after repeatedly bending the sample inward and outward. As clearly seen in Fig. 6b, the present Au mesh exhibits an almost invariant resistance which is comparable to that of the continuous film even after bending for 500 times. The present results reveal that the ultra-thin Au nanomesh can be a promising candidate as an electrode for flexible electronic devices.

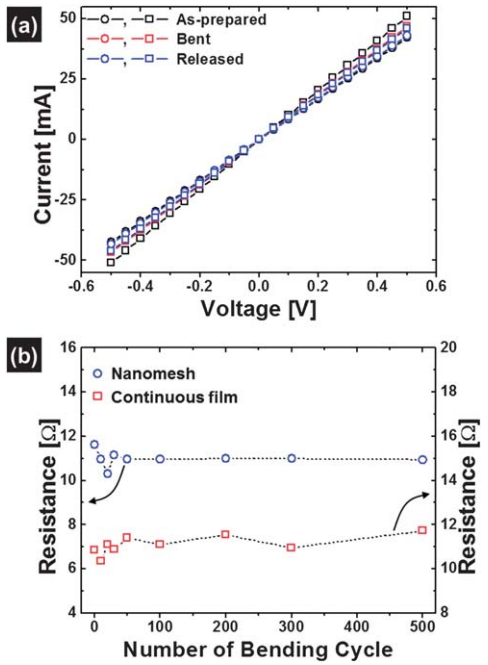

Fig. 6 (a) *I–V* curves measured from an Au nanomesh and a continuous Au film on a PET substrate at different bending states; as-prepared, bent, and released. Circular and square symbols represent *I–V* characteristics of the Au mesh and the continuous Au film, respectively. (b) Variation in the resistance of the Au mesh and the continuous film after bending for different numbers of cycle from 0 to 500. One bending cycle was performed by sequentially bending samples inward and outward. The dashed line is added as a guide to the eye.

Table 1 Resistances of Au nanomeshes and continuous Au thin films measured at different bending states; as-prepared, bent, and released (unit: Ω)

	As-prepared	Bent	Released
Au mesh	11.8	11.6	11.6
Continuous Au film	9.82	10.66	10.87

Conclusions

We have developed a convenient method for the fabrication of the versatile ultra-thin Au nanomesh with hexagonally ordered arrays of nanoholes by utilizing a reusable free-standing anodic aluminium oxide (AAO) membrane as a replication master. Multiple copies of Au nanomeshes were replicated from a single AAO membrane by selective removal of a thin sacrificial Ag layer from Au/Ag-coated AAO. In our process, the AAO membrane can be reused more than 30 times. Therefore, the present approach for the fabrication of Au nanomeshes is economical in terms of time and cost in comparison to conventional lithography-based methods. We also demonstrated the versatility of the Au nanomesh as a starting material for fabricating various nanostructures. Au nanomeshes were utilized not only as a metal catalyst for fabricating well-ordered Si nanowire arrays through metal-assisted chemical etching (MaCE) of silicon wafer, but also as a lithographic mask for pattering of the polymeric film with sub-100 nm resolution. Our nanopatterning method using a metal mask can be applied to an arbitrary substrate by simply adopting the appropriate materials and etching conditions. In addition, the Au mesh, transferred on a flexible substrate, *i.e.*, polyethylene terephthalate (PET), exhibited comparable resistance values to a continuous Au thin film irrespective of its bending state, indicating the promising application capability of the ultra-thin Au mesh as an electrode material for flexible electronic devices. It is expected that the present fabrication method of metal nanomeshes can be readily extended to other materials systems that have potential application in plasmonics (*e.g.*, surface-enhanced Raman spectroscopy) or photo-electronics (*e.g.*, transparent and flexible electrodes).

Acknowledgements

This work was supported by Future-based Technology Development Program (Nano Fields) through the National Research Foundation of Korea (NRF) funded by the Ministry of Education, Science and Technology (Grant no. 2010-0029332).

Notes and references

1 J. Henzie, M. H. Lee and T. W. Odom, *Nat. Nanotechnol.*, 2007, **2**, 549–554.
2 J. Henzie, J. Lee, M. H. Lee, W. Hasan and T. W. Odom, *Annu. Rev. Phys. Chem.*, 2009, **60**, 147–165.
3 J. W. Menezes, J. Ferreira, M. J. L. Santos, L. Cescato and A. G. Brolo, *Adv. Funct. Mater.*, 2010, **20**, 3918–3924.
4 C. Ke, C. Zhonggang, L. Qianqian, W. Shujie and D. Zuliang, *Nanotechnology*, 2012, **23**, 425303.
5 H. A. Atwater and A. Polman, *Nat. Mater.*, 2010, **9**, 205–213.

6 K. Nakamoto, R. Kurita and O. Niwa, *Anal. Chem.*, 2012, **84**, 3187–3191.
7 T. Sannomiya, O. Scholder, K. Jefimovs, C. Hafner and A. B. Dahlin, *Small*, 2011, **7**, 1653–1663.
8 N. P. Westcott, Y. Lou, J. F. Muth and M. N. Yousaf, *Langmuir*, 2009, **25**, 11236–11238.
9 S.-W. Chang, V. P. Chuang, S. T. Boles, C. A. Ross and C. V. Thompson, *Adv. Funct. Mater.*, 2009, **19**, 2495–2500.
10 J. Kim, H. Han, Y. H. Kim, S.-H. Choi, J.-C. Kim and W. Lee, *ACS Nano*, 2011, **5**, 3222–3229.
11 J. Kim, H. Rhu and W. Lee, *J. Mater. Chem.*, 2011, **21**, 15889–15894.
12 J. Kim, Y. H. Kim, S.-H. Choi and W. Lee, *ACS Nano*, 2011, **5**, 5242–5248.
13 Q. Yu, P. Guan, D. Qin, G. Golden and P. M. Wallace, *Nano Lett.*, 2008, **8**, 1923–1928.
14 M. Haupt, S. Miller, R. Glass, M. Arnold, R. Sauer, K. Thonke, M. Möller and J. P. Spatz, *Adv. Mater.*, 2003, **15**, 829–831.
15 J. W. Diggle, T. C. Downie and C. W. Goulding, *Chem. Rev.*, 1969, **69**, 365–405.
16 W. Lee, R. Ji, U. Gosele and K. Nielsch, *Nat. Mater.*, 2006, **5**, 741–747.
17 Y. Lei, W. Cai and G. Wilde, *Prog. Mater. Sci.*, 2007, **52**, 465–539.
18 A. M. Md Jani, D. Losic and N. H. Voelcker, *Prog. Mater. Sci.*, 2013, **58**, 636–704.
19 H. Han, S.-J. Park, J. S. Jang, H. Ryu, K. J. Kim, S. Baik and W. Lee, *ACS Appl. Mater. Interfaces*, 2013, **5**, 3441–3448.
20 J. W. Elam, D. Routkevitch, P. P. Mardilovich and S. M. George, *Chem. Mater.*, 2003, **15**, 3507–3517.
21 Y. Lei and W.-K. Chim, *Chem. Mater.*, 2005, **17**, 580–585.
22 W. Lee, M. Alexe, K. Nielsch and U. Gösele, *Chem. Mater.*, 2005, **17**, 3325–3327.
23 Q. Lin, B. Hua, S.-f. Leung, X. Duan and Z. Fan, *ACS Nano*, 2013, **7**, 2725–2732.
24 R. L. Smith and S. D. Collins, *J. Appl. Phys.*, 1992, **71**, R1–R22.
25 B.-J. Kim, Y. Cho, M.-S. Jung, H.-A. S. Shin, M.-W. Moon, H. N. Han, K. T. Nam, Y.-C. Joo and I.-S. Choi, *Small*, 2012, **8**, 3300–3306.